Electrochemiluminescence Imaging

DOI: 10.1002/anie.201203815

Imaging Latent Fingerprints by Electrochemiluminescence**

*Linru Xu, Yan Li, Suozhu Wu, Xianghong Liu, and Bin Su**

Fingerprints are impressions of the friction ridge pattern left by human fingertips after touching a surface. They function as an indispensable tool in forensic investigations and personal identification, as well as in our daily life for many other purposes, such as safety inspection, access control, and individual credentials.[1] Fingerprints are composed of perspiration, natural secretion residue, and exogenous components from the environment, some of which are rarely seen (termed invisible or latent fingerprints, LFPs) and require some means of "development" by applying external materials to enhance their visualization. To date, innumerable methods, including both chemical and physical treatments, have been exploited for LFP detection.[1a,2] Additionally, research interest has been recently directed to identifying drugs and drug metabolites, explosive residues, or other secretion chemicals in LFPs.[2d,e,g,3]

Among various methods, electrochemical approaches have recently attracted considerable attention. For example, combining electrochemistry with the surface-plasmon resonance spectroscopy allows a fast and sensitive visualization of fingerprint and detection of explosive residues.[3f] Scanning electrochemical techniques, including scanning Kelvin probe[4] and scanning electrochemical microscopes,[2i,5] have also been applied for imaging fingerprint on the basis of the spatial difference in the surface work function and electrochemical reactivity. Selective electrodeposition of conducting polymers on electrode surfaces is also able to enhance the fingerprint visualization by the electrochromic effect.[2h,6] Herein we report an alternative attempt to enhance the visualization of LFPs by electrochemiluminescence (ECL).

ECL, where a chemiluminescence is initiated and controlled by applying a potential, has grown significantly as a highly sensitive and selective analytical and diagnostic method in recent years.[7] As the light-emitting species are generated in situ close to electrode surfaces, ECL reflects the local surface reactivity, has a near-zero background and allows temporal and spatial control over the reaction. These features make ECL very useful in imaging applications, for example for the examination of the functional areas of electrodes,[8] the distribution of electrochemical active sites[9] and the electron-transfer kinetics,[10] for scanning sample surfaces with an ultramicroelectrode tip generating ECL as a light source,[11] and for building light-emitting and displaying devices.[12] Chemical sensors or microarray sensors based on ECL imaging have also been developed,[13] for example for detection in microelectrochemical and microfluidic systems,[14] and for screening metabolite-generated toxicity and detecting cancer biomarker proteins.[15]

Herein, we have demonstrated that the spatially selective control of ECL generation on the electrode surface is an effective means of visualizing LFPs. Figure 1a shows an experimental system for this purpose (see also the Supporting Information, Figure S1). An electrode, indium tin oxide (ITO)-covered glass or stainless steel sheet, bearing a fingerprint was placed in a cell positioned in a dark box with a silver/silver chloride (Ag/AgCl/3 M KCl) and a platinum wire ring as the reference and counter electrode, respectively. When a suitable voltage is applied with a conventional potentiostat, ECL was generated and captured by a sensitive CCD camera. In principle, the fingerprint functions as a mask or template, and its visualization can be enhanced by spatially controlling the ECL generation either from the bare surface or from the ridge details. These two modes are designated negative and positive imaging, respectively (Figure 1b,c).

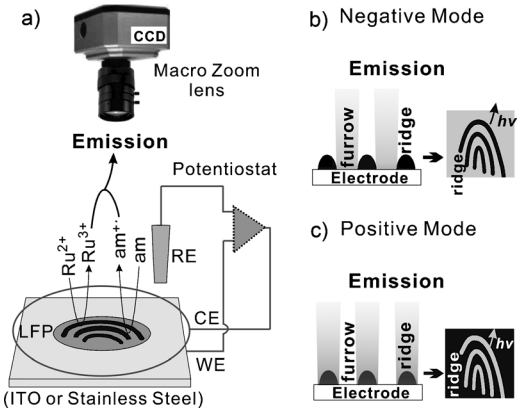

Figure 1. a) The ECL imaging system: Ru^{2+} and am represent the ECL-generating luminophore and the amine co-reactant, respectively. b,c) The imaging strategy for visualizing LPFs in the negative (b) and positive (c) mode.

The negative-imaging mode was performed by directly exposing the electrode bearing a sebaceous (sebum-rich) fingerprint to the solution containing tris(2,2′-bipyridyl) ruthenium(II) ($[Ru(bpy)_3]^{2+}$) and tri-*n*-propylamine (TPrA). The ridge deposit of a sebaceous fingerprint comprises a complex mixture of perspiration and natural secretion residues, such as fatty acids, phospholipids, wax esters, sterols, squalene,[1a] which make the underlying surface electrochemically inert or less active, thereby inhibiting the electrochem-

[*] L. R. Xu, Y. Li, S. Z. Wu, X. H. Liu, Dr. B. Su
Institute of Microanalytical Systems, Department of Chemistry
Zhejiang University, Hangzhou 310058 (China)
E-mail: subin@zju.edu.cn
Homepage: http://mypage.zju.edu.cn/binsu

[**] This work is supported by the National Natural Science Foundation of China (21005071) and Z.J.U.

Supporting information for this article is available on the WWW under http://dx.doi.org/10.1002/anie.201203815.

ical activity. In contrast, on the bare surface uncovered by the fingerprint, the ECL reaction could proceed by the well-known co-reactant pathway when applying a suitable positive voltage (for the mechanism, see the Supporting Information). Eventually, the light emission was only generated from the bare electrode surface including the furrows between the papillary ridges, producing a negative image of the fingerprint (Figure 1b).

Figure 2 shows a representative fingerprint enhanced in the negative-imaging manner. Compared to the bright-field image (Figure 2a), the ECL image (Figure 2b) displays a clearly resolved spatial pattern of a sebaceous fingerprint in which the dark ridge deposits contrasted remarkably with the bright substrate for visualization. The second-level detail, including the ridge termination, lake, bifurcation, and crossover, could be recognized. These second-level characteristics in principle form the basis of fingerprint identification, and their unambiguous imaging is critical in practical identification. The third-level detail, namely the sweat pores from which the sweat is secreted, was also clearly observed along the ridges. Seeing these details can be ascribed to the fact that ECL exactly reflects the local electrochemical activity of electrode surface. In conventional methods involving application of external materials, the ridges become decorated so that the third-level detail is often difficult to see. The third-level detail is used by forensic officers in some countries for confirmation of an identification match. It can effectively assist the holistic identification and in particular has promise for partial fingerprints or other cases with a lack of unambiguous second-level detail.

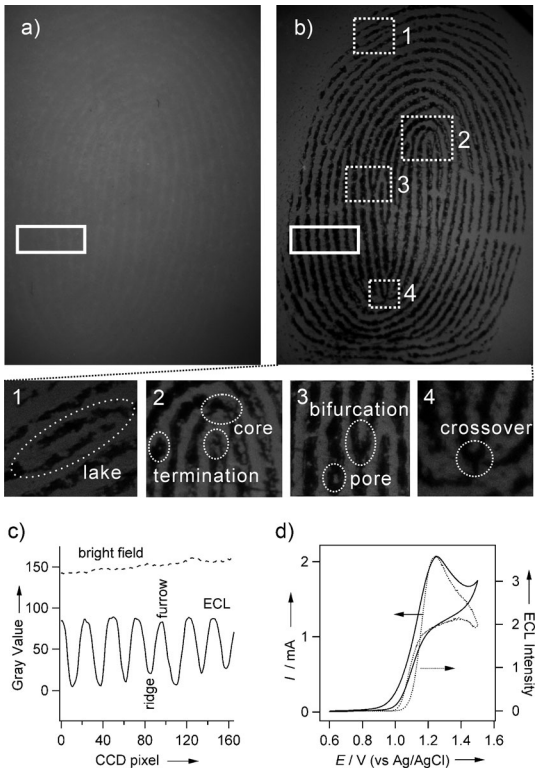

Figure 2. a) Bright-field image of a sebaceous fingerprint deposited on an ITO electrode. b) ECL image obtained in the negative mode at an applied potential of 1.13 V and in 0.01 M phosphate buffer solution (pH 7.4, sodium salts) containing 0.5 mM $[Ru(bpy)_3]^{2+}$ as ECL-generating luminophore and 50 mM TPrA as co-reactant. In the ECL image, the second- and third-level details can be identified. c) Cross-sectional gray values over seven parallel ridges as indicated by the white rectangles in (a) and (b). d) Simultaneous cyclic voltammetry (——) and ECL emission profile (•••••) of an ITO electrode deposited with a sebaceous fingerprint at a potential scan rate of 0.05 Vs^{-1}.

The visualization enhancement by ECL was confirmed by scrutinizing the cross-sectional gray values over a few parallel ridges. As shown in Figure 2c, in the bright-field image the cross-sectional gray value over seven parallel ridges varies negligibly, while that changes significantly from ridge to furrow in the ECL image. The dark ridge defines a smaller gray value, while the bright furrow defines a larger value. The average difference in the gray value is about 70, suggesting that the fingerprint visualization was enhanced by several tens of times by in situ ECL generation.

The negative image was obtained by applying a constant potential of +1.13 V optimized by examination of the image with respect to the emission-voltage profile. As shown in Figure 2d, the quality of ECL images coincides well with the current and emission profile (Supporting Information, Figure S2), confirming that the visualization enhancement indeed arises from ECL generation. In the similar manner, the concentration of $[Ru(bpy)_3]^{2+}$ for a satisfactory enhancement was determined to be 0.5 mM (Supporting Information, Figure S3). With these two parameters, the ECL image obtained was relatively stable in about 40 s (Supporting Information, Figure S4). The decay of image quality at a longer time is most probably due to the significant consumption of TPrA. Once transferring the electrode to fresh $[Ru(bpy)_3]^{2+}$/TPrA solutions, the ECL image can be repeatedly observed (Supporting Information, Figure S5). This is due to the non-destructive nature of this method, which does not rely on any pre-/post-treatment.

Non-destructive imaging and developing LFPs without any pre-treatment is one of important aspects of current research activities, but methods that fulfill this purpose are few.[2f–h,3f,4a,6,16] The ECL imaging in a negative manner is apparently a simple yet effective approach. Indeed, not only fresh LFPs but also aged LFPs can be visually enhanced. As shown in Figure 3, the ridge pattern of two- and seven-month-old sebaceous fingerprints can be clearly identified. More interestingly, the third-level detail, namely sweat pores, can be much more clearly resolved along the ridges. Furthermore, the negative imaging also works well in other ECL reaction systems, such as that involving a luminol–hydrogen peroxide pair, as well as on other conducting substrates, such as stainless steel plates (Supporting Information, Figures S6, S7).

The second imaging method, termed the positive mode, was conducted after tagging the fingerprint ridge deposit with ECL-generating luminophores. The immobilized luminophores can then react with freely diffusing co-reactants to generate ECL. In this case, the papillary ridges, instead of the furrows in the negative imaging mode, were illuminated and contrasted with the dark substrate sufficiently, eventually generating a positive image of the fingerprint (see the mechanism diagram in Figure 1c). Given that amino acids are one of predominant species in the eccrine sweat,[1a]

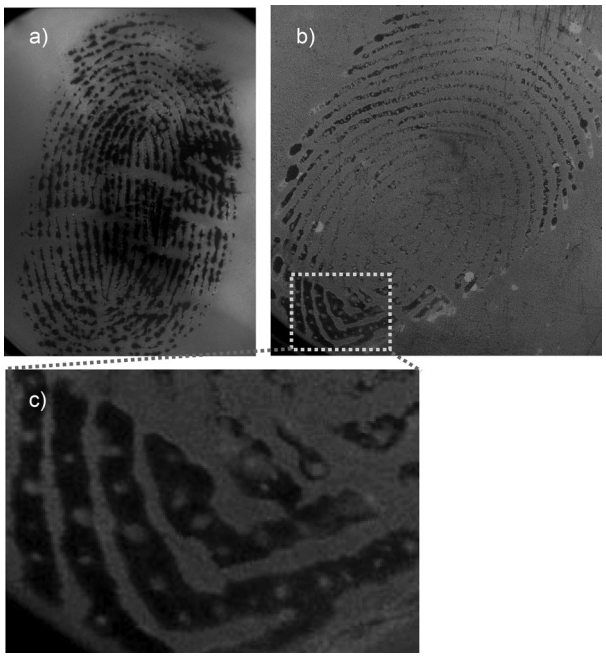

Figure 3. a, b) ECL images of a two-month-old and seven-month-old sebaceous fingerprints deposited on ITO electrodes. c) Magnified image showing sweat pores visualized along the ridges.

ruthenium bis(2,2′-bipyridine) (2,2′-bipyridine-4,4′-dicarboxylic acid) *N*-hydroxysuccinimide ester ([Ru(bpy)$_2$(dcbpy)NHS]) was used to functionalize the fingerprint ridges by the formation of amide bonds (Figure 4a).

Figure 4b shows an example of ECL images thus developed for sebaceous fingerprints by applying a constant potential of +1.3 V (optimized by examination of the image with respect to the emission-voltage profile; Supporting Information, Figures S8, S9) and using 2-(dibutylamino) ethanol (DBAE) as the co-reactant. Apparently, the ridges are illuminated by ECL and contrasted sufficiently with the dark substrate for visualization. In this image, the second-level detail, including the ridge termination and bifurcation, can be also recognized. In contrast, under daylight the fingerprint before and after tagging treatment is hardly seen by the naked eye (Figure 4c). Even under UV illumination, only a faint photoluminescence image (as shown in Figure 4d) was obtained with locally distributed bright fragments, which could not reflect the overall fingerprint pattern. A poor photoluminescence image can be possibly ascribed to the aggregation-caused quenching, considering the short-range interaction between ruthenium luminophores immobilized on the ridges. Although the similar quenching cannot be excluded either in the ECL reaction, it might be less effective considering the ECL reaction takes place between immobilized luminophores and dissolved co-reactants. Another key advantage of ECL over light-induced emission is that external light stimulation is not required, thus having low background interference.

The covalent interaction of [Ru(bpy)$_2$(dcbpy)NHS] with fingerprint deposits by the NHS group was confirmed by mass spectrometric measurements (Supporting Information, Figure S10), as well as two control experiments. First, when

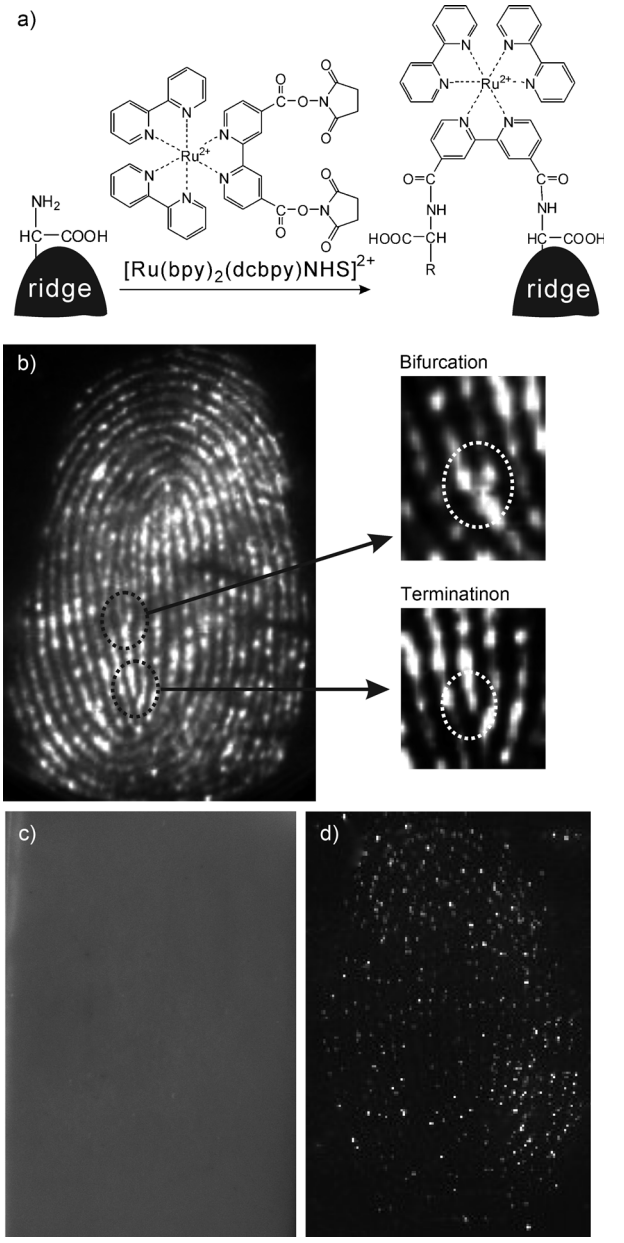

Figure 4. a) Mechanism illustration of tagging fingerprint ridges with ECL-generating luminophores. b–d) ECL (b), bright-field (c), and photoluminescence (d) images of a sebaceous fingerprint after incubation with freshely prepared [Ru(bpy)$_2$(dcbpy)NHS] solution for 1 h. The ECL image was obtained at an applied potential of 1.3 V in 0.01 M phosphate buffer solution (pH 7.4) containing 50 mM 2-(dibutylamino) ethanol (DBAE) as the co-reactant. The photoluminescence image was acquired using a 460 nm excitation light source and a 600 nm long-pass filter.

treating the fingerprints with two other ruthenium coordination compounds, [Ru(bpy)$_3$Cl$_2$] and [Ru(bpy)$_2$(dcbpy)](PF$_6$)$_2$, no ECL enhancement was observed (Supporting Information, Figure S11). Second, at least 30 min of incubation with the [Ru(bpy)$_2$(dcbpy)NHS] solution was required to obtain a satisfied ECL image (Supporting Information, Figure S12), which is in good agreement with the typical reaction time between NHS and primary amine group for the formation of

amide bond.[17] However, these data could not rule out the possibility of physical adsorption of [Ru(bpy)$_2$(dcbpy)NHS] on the ridge deposits by the hydrophobic interaction. Nevertheless, similar enhancement effect observed for eccrine fingerprints (Supporting Information, Figure S13) indicated that the physical adsorption is probably much less effective, given the predominant species in eccrine fingerprints are inorganic salts as well as amino acids and lipids.[1a]

In summary, we have exploited two operating methods for visualizing LFPs on the basis of spatially selective control of ECL generation at the electrode surface. The negative mode represents a direct, rapid, simple and non-destructive method that is suitable for enhancing the visualization of sebaceous LFPs, aged LFPs, as well as identifying the second- and third-level characteristic details. It does not involve any pre-/post-treatment that is usually laborious but necessary in most of current detection methods. Also, it is safe for examiners when comparing with those using fume or dust-brushing treatment. In the case of the positive mode, the absence or lower levels of aggregation-caused luminescence quenching is its important advantage over light-excited emission. Moreover, it has promise for detecting secreted metabolites in the fingerprint in conjunction with immunolabeling methodologies for diagnostic purposes.[2d,e,3a–e,18] Furthermore, if ECL is particularly suited for conductive substrates, simple chemiluminescence should be equally feasible for non-conductive ones, for example by tagging the ridges with a luminophore that could be chemically switched.

Received: May 17, 2012
Published online: July 2, 2012

Keywords: electrochemiluminescence imaging · fingerprints · ridge details · spatial control · visualization enhancement

[1] a) H. C. Lee, R. E. Gaensslen, *Advances in Fingerprint Technology*, 2nd ed., CRC, Boca Raton, **2001**; b) M. R. Hawthorne, *Fingerprint Analysis and Understanding*, CRC, Boca Raton, **2009**; c) C. Champod, C. Lennard, P. Margot, M. Stoilovic, *Fingerprints and Other Ridge Skin Impressions*, CRC, Boca Raton, **2004**.

[2] a) V. Bowman, *Fingerprint Development Handbook*, 2nd ed., Heanor Gate Printing Limited: Heanor, Derbyshire, UK, **2005**; b) P. Hazarika, D. A. Russell, *Angew. Chem.* **2012**, *124*, 3582 – 3589; *Angew. Chem. Int. Ed.* **2012**, *51*, 3524 – 3531; c) M. Sametband, I. Shweky, U. Banin, D. Mandler, J. Almog, *Chem. Commun.* **2007**, 1142 – 1144; d) P. Hazarika, S. M. Jickells, K. Wolff, D. A. Russell, *Angew. Chem.* **2008**, *120*, 10321 – 10324; *Angew. Chem. Int. Ed.* **2008**, *47*, 10167 – 10170; e) X. Spindler, O. Hofstetter, A. M. McDonagh, C. Roux, C. Lennard, *Chem. Commun.* **2011**, *47*, 5602 – 5604; f) J. S. Day, H. G. M. Edwards, S. A. Dobrowski, A. M. Voice, *Spectrochim. Acta Part A* **2004**, *60*, 563 – 568; g) D. R. Ifa, N. E. Manicke, A. L. Dill, R. G. Cooks, *Science* **2008**, *321*, 805; h) A. L. Beresford, A. R. Hillman, *Anal. Chem.* **2010**, *82*, 483 – 486; i) M. Q. Zhang, A. Becue, M. Prudent, C. Champod, H. H. Girault, *Chem. Commun.* **2007**, 3948 – 3950.

[3] a) R. Leggett, E. E. Lee-Smith, S. M. Jickells, D. A. Russell, *Angew. Chem.* **2007**, *119*, 4178 – 4181; *Angew. Chem. Int. Ed.* **2007**, *46*, 4100 – 4103; b) P. Hazarika, S. M. Jickells, D. A. Russell, *Analyst* **2009**, *134*, 93 – 96; c) P. Hazarika, S. M. Jickells, K. Wolff, D. A. Russell, *Anal. Chem.* **2010**, *82*, 9150 – 9154; d) A. M. Boddis, D. A. Russell, *Anal. Methods* **2011**, *3*, 519 – 523; e) A. M. Boddis, D. A. Russell, *Anal. Methods* **2012**, *4*, 637 – 641; f) X. N. Shan, U. Patel, S. P. Wang, R. Iglesias, N. J. Tao, *Science* **2010**, *327*, 1363 – 1366.

[4] a) G. Williams, N. McMurray, *Forensic Sci. Int.* **2007**, *167*, 102 – 109; b) G. Williams, N. McMurray, D. A. Worsley, *J. Forensic Sci.* **2001**, *46*, 1085 – 1092.

[5] a) M. Q. Zhang, H. H. Girault, *Electrochem. Commun.* **2007**, *9*, 1778 – 1782; b) M. Q. Zhang, H. H. Girault, *Analyst* **2009**, *134*, 25 – 30; c) G. Qin, M. Zhang, T. Zhang, Y. Zhang, M. McIntosh, X. Li, X. Zhang, *Electroanalysis* **2012**, *24*, 1027 – 1032.

[6] a) C. Bersellini, L. Garofano, M. Giannetto, F. Lusardi, G. Mori, *J. Forensic Sci.* **2001**, *46*, 871 – 877; b) A. L. Beresford, R. M. Brown, A. R. Hillman, J. W. Bond, *J. Forensic Sci.* **2012**, *57*, 93 – 102; c) R. M. Rachel, A. R. Hillman, *Phys. Chem. Chem. Phys.* **2012**, *14*, 8653 – 8661.

[7] a) W. Miao, *Chem. Rev.* **2008**, *108*, 2506 – 2553; b) M. Richter, *Chem. Rev.* **2004**, *104*, 3003 – 3036; c) A. J. Bard, J. Debad, J. Leland, G. Sigal, J. Wilbur, J. Wohlstadter, in *Encyclopedia of Analytical Chemistry: Applications, Theory, and Instrumentation*, *Vol. 11* (Ed.: R. A. Meyers), Wiley, Chichester, **2000**, p. 9842; d) A. J. Bard, *Electrogenerated Chemiluminescence*, Marcel Dekker, New York, **2004**; e) L. Z. Hu, G. B. Xu, *Chem. Soc. Rev.* **2010**, *39*, 3275 – 3304; f) H. P. Huang, J. J. Li, J. J. Zhu, *Anal. Methods* **2011**, *3*, 33 – 42.

[8] a) R. C. Engstrom, C. M. Pharr, M. D. Koppang, *J. Electroanal. Chem.* **1987**, *221*, 251 – 255; b) C. M. Pharr, R. C. Engstrom, R. A. Tople, T. K. Bee, P. L. Unzelman, *J. Electroanal. Chem.* **1989**, *278*, 119 – 128; c) R. M. Wightman, C. L. Curtis, P. A. Flowers, R. G. Maus, E. M. McDonald, *J. Phys. Chem. B* **1998**, *102*, 9991 – 9996; d) R. G. Maus, E. M. McDonald, R. M. Wightman, *Anal. Chem.* **1999**, *71*, 4944 – 4950.

[9] a) R. C. Engstrom, K. W. Johnson, S. Desjarlais, *Anal. Chem.* **1987**, *59*, 670 – 673; b) R. J. Bowling, R. L. McCreery, C. M. Pharr, R. C. Engstrom, *Anal. Chem.* **1989**, *61*, 2763 – 2766; c) P. Hopper, W. G. Kuhr, *Anal. Chem.* **1996**, *68*, 1996 – 2004; d) S. Szunerits, J. M. Tam, L. Thouin, C. Amatore, D. R. Walt, *Anal. Chem.* **2003**, *75*, 4382 – 4388; e) K. Honda, T. Noda, A. Yoshimura, K. Nakagawa, A. Fujishima, *J. Phys. Chem. B* **2004**, *108*, 16117 – 16127.

[10] Y. L. Chang, R. E. Palacios, F. R. F. Fan, A. J. Bard, P. F. Barbara, *J. Am. Chem. Soc.* **2008**, *130*, 8906 – 8907.

[11] a) F. R. F. Fan, D. Cliffel, A. J. Bard, *Anal. Chem.* **1998**, *70*, 2941 – 2948; b) Y. B. Zu, Z. F. Ding, J. F. Zhou, Y. M. Lee, A. J. Bard, *Anal. Chem.* **2001**, *73*, 2153 – 2156; c) R. G. Maus, R. M. Wightman, *Anal. Chem.* **2001**, *73*, 3993 – 3998; d) F. R. F. Fan, A. J. Bard, *J. Phys. Chem. B* **2003**, *107*, 1781 – 1787; e) R. Lei, L. Stratmann, D. Schafer, T. Erichsen, S. Neugebauer, N. Li, W. Schuhmann, *Anal. Chem.* **2009**, *81*, 5070 – 5074.

[12] a) Y. L. Chang, R. E. Palacios, J. T. Chen, K. J. Stevenson, S. Guo, W. M. Lackowski, P. F. Barbara, *J. Am. Chem. Soc.* **2009**, *131*, 14166 – 14167; b) S. Guo, O. Fabian, Y. L. Chang, J. T. Chen, W. M. Lackowski, P. F. Barbara, *J. Am. Chem. Soc.* **2011**, *133*, 11994 – 12000.

[13] a) E. S. Jin, B. J. Norris, P. Pantano, *Electroanalysis* **2001**, *13*, 1287 – 1290; b) A. Chovin, P. Garrigue, P. Vinatier, N. Sojic, *Anal. Chem.* **2004**, *76*, 357 – 364; c) F. Deiss, C. N. LaFratta, M. Symer, T. M. Blicharz, N. Sojic, D. R. Walt, *J. Am. Chem. Soc.* **2009**, *131*, 6088 – 6089; d) Z. J. Lin, X. M. Chen, T. T. Jia, X. D. Wang, Z. X. Xie, M. Oyama, X. Chen, *Anal. Chem.* **2009**, *81*, 830 – 833; e) L. S. Dolci, S. Zanarini, L. Della Ciana, F. Paolucci, A. Roda, *Anal. Chem.* **2009**, *81*, 6234 – 6241; f) J. L. Delaney, C. F. Hogan, J. F. Tian, W. Shen, *Anal. Chem.* **2011**, *83*, 1300 – 1306.

[14] a) W. Zhan, J. Alvarez, R. M. Crooks, *J. Am. Chem. Soc.* **2002**, *124*, 13265 – 13270; b) W. Zhan, R. M. Crooks, *J. Am. Chem. Soc.*

2003, *125*, 9934 – 9935; c) K. F. Chow, F. Mavre, R. M. Crooks, *J. Am. Chem. Soc.* **2008**, *130*, 7544 – 7545; d) K. F. Chow, F. Mavre, J. A. Crooks, B. Y. Chang, R. M. Crooks, *J. Am. Chem. Soc.* **2009**, *131*, 8364 – 8365; e) F. Mavré, R. K. Anand, D. R. Laws, K. F. Chow, B. Y. Chang, J. A. Crooks, R. M. Crooks, *Anal. Chem.* **2010**, *82*, 8766 – 8774; f) S. E. Fosdick, J. A. Crooks, B. Y. Chang, R. M. Crooks, *J. Am. Chem. Soc.* **2010**, *132*, 9226 – 9227.

[15] a) E. G. Hvastkovs, M. So, S. Krishnan, B. Bajrami, M. Tarun, I. Jansson, J. B. Schenkman, J. F. Rusling, *Anal. Chem.* **2007**, *79*, 1897 – 1906; b) S. Krishnan, E. G. Hvastkovs, B. Bajrami, I. Jansson, J. B. Schenkman, J. F. Rusling, *Chem. Commun.* **2007**, 1713 – 1715; c) S. Krishnan, E. G. Hvastkovs, B. Bajrami, D. Choudhary, J. B. Schenkman, J. F. Rusling, *Anal. Chem.* **2008**, *80*, 5279 – 5285; d) S. M. Pan, L. L. Zhao, J. B. Schenkman, J. F. Rusling, *Anal. Chem.* **2011**, *83*, 2754 – 2760; e) N. P. Sardesai, J. C. Barron, J. F. Rusling, *Anal. Chem.* **2011**, *83*, 6698 – 6703.

[16] F. Cortés-Salazar, D. Momotenko, H. H. Girault, A. Lesch, G. Wittstock, *Anal. Chem.* **2011**, *83*, 1493 – 1499.

[17] G. F. Blackburn, H. P. Shah, J. H. Kenten, J. Leland, R. A. Kamin, J. Link, J. Peterman, M. J. Powell, A. Shah, D. B. Talley, S. K. Tyagi, E. Wilkins, T. G. Wu, R. J. Massey, *Clin. Chem.* **1991**, *37*, 1534 – 1539.

[18] O. S. Wolfbeis, *Angew. Chem.* **2009**, *121*, 2302 – 2304; *Angew. Chem. Int. Ed.* **2009**, *48*, 2268 – 2269.

